ELECTRICAL RESISTANCE OF MUSCLE CAPILLARY ENDOTHELIUM

SØREN-PETER OLESEN AND CHRISTIAN CRONE
Institute of Medical Physiology, Department A, University of Copenhagen, The Panum Institute, DK-2200 Copenhagen N., Denmark

ABSTRACT A recently developed technique for in vivo determination of the electrical resistance of vascular endothelium in microvessels was applied to the vessels in a thin frog muscle, *m. cutaneus pectoris*. The technique consists of injection of current via a glass micropipette into a capillary and measurement of the resulting intra- and extravascular potential profiles with another micropipette placed at various distances from the current source. The theory of Peskoff and Eisenberg (1974) was used to handle the problems arising from distributed extravascular resistances and was experimentally shown to describe the external field satisfactorily. With this extension of one-dimensional cable theory the specific electrical resistance of arterial microvessels was 33 Ωcm^2 and of venous capillaries 23 Ωcm^2. The "length constants" were 135 and 112 μm, respectively. If results from arterial and venous vessels are taken together, the ionic permeabilities at 20°C were $P_{Na} = 3.9 \times 10^{-5}$ cm · s^{-1}, $P_K = 5.7 \times 10^{-5}$ cm · s^{-1}, $P_{Cl} = 5.9 \times 10^{-5}$ cm · s^{-1} and $P_{HCO_3} = 3.4 \times 10^{-5}$ cm · s^{-1}. These figures agree with figures for capillary permeability obtained in tracer experiments on whole muscle. The study bridges a gap between single capillary and whole organ techniques with the conclusion that the two different approaches lead to similar results in muscle capillaries.

INTRODUCTION

The capillary wall in skeletal muscle has played a significant role in the exploration of capillary physiology ever since the time of Krogh who used it as a paradigm for the concept of a tissue cylinder being supplied from a central capillary (Krogh, 1919). Later, the first quantitative determinations of capillary permeability were carried out on skeletal muscle capillaries (Pappenheimer et al., 1951; Pappenheimer, 1953) and the pore theory grew out of these studies. The early permeability values have sometimes been questioned and although many studies have been carried out on skeletal muscle some doubt remains concerning the true permeabilities to low molecular weight hydrophilic solutes (Renkin and Curry, 1978, Crone and Levitt, in press). The primary source of uncertainty in permeability values in whole organs is the value of surface area through which diffusion takes place. In skeletal muscle the assessment of capillary surface area is particularly difficult because the number of perfused capillaries may vary depending on the metabolic rate of the tissue (Renkin et al., 1966; Paaske, 1977; Hudlicka et al., 1982). Also heterogeneity of perfusion (Tyml et al., 1981) limits great precision in permeability determination because diffusion may be flow limited in some capillaries and not in others. Some investigators study fully dilated capillary beds, whilst others have been working on unmedicated preparations. For these and other reasons alternative approaches to capillary permeability in muscle are needed. The advantage of single capillary techniques is that many of the problems connected with whole organ approaches are avoided. This paper reports studies on single muscle capillaries with a newly developed electrophysiological technique which allows determination of the DC-resistance of the endothelium. Because the current is carried largely by Na^+, Cl^-, HCO_3^-, and K^+ the results can be interpreted in terms of small solute permeability.

THEORY

The basic theory behind determination of capillary wall resistance is the theory for "leaky cables" developed by Hodgkin and Rushton (1946). According to this theory, membrane resistance can be determined under certain limiting conditions if current can be injected into a cylindrical structure surrounded by a high resistance membrane, the whole structure being submerged in well-conducting saline solution containing the ground leads. When applied to capillaries the elementary theory must be extended and shaped according to the special conditions in different tissues. A prominent problem concerns the conductivity of the medium in which the capillaries are situated in vivo. Specifically, the conductance of the tissues is far from negligible and the configuration of the external electrical field must be taken into account to extract the wall resistance from the measurements of the intracapillary potential profile in response to current injections.

Under ideal conditions (isotropic, well-conducting external medium) the one-dimensional potential profile within a leaky cable in response to a DC-step is

$$V(x) = V(0) \exp(-x/\lambda), \quad (1)$$

where x is the axial distance from the current source. λ, the length constant, is equal to $\sqrt{r_m/r_i}$, where r_m is the membrane resistance per centimeter of capillary length, and r_i is the internal resistance per centimeter of capillary length. $r_i = \rho_i/\pi a^2$, where ρ_i is the specific

resistivity of capillary blood, and a is the radius. Because the specific membrane resistance, R_m, is equal to $2\pi a r_m$, it follows that

$$R_m = r_i \cdot \lambda^2 \cdot 2\pi a. \quad (2)$$

Thus, under ideal conditions, the specific membrane resistance can be calculated if the length constant can be experimentally determined when current is injected into the capillary.

The capillaries at the surface of the frog brain come close to ideal conditions, and their electrical resistance was determined according to Eq. 2 by Crone and Olesen (1982). On the other hand the topological conditions of the frog mesenteric capillary were such as to require an extensive theoretical treatment to determine their electrical characteristics (Crone and Christensen, 1981).

Because capillaries in muscle tissue lie buried between cells and are not in free suspension it follows that the experimental situation must be carefully analyzed and, as shown in Appendix A, a rather involved mathematical treatment is required to extract wall resistance from the intracapillary potential profile. The reader is referred to Appendix A for a detailed account of the system as we interpret it, and only the essential points are given here.

The fact that the distributed electrical resistance outside a capillary is of a magnitude comparable to that of the endothelium means that the potential on the outside does not fall to zero or near zero, but that it represents a significant fraction of the potential difference across the capillary wall (in response to intracapillary current injection). The field outside the experimental vessel is shaped by the intracapillary potential that decays axially in the two directions away from the current source because current leaks out into the external medium all along the capillary. We have modeled the problem based upon a theory developed by Peskoff and Eisenberg (1973, 1974) for a point source in a leaky cable surrounded by a medium of finite conductivity. One may argue that muscle tissue is not isotropic, but, as will be documented experimentally, the error committed by ignoring tissue anisotropy is tolerable, which may partly be explained by the fact that the superfusate that covers the experimental muscle also contributes to the external resistance.

The result of the analysis is given in Appendix A in a general form. Besides capillary wall resistance the internal potential contour depends on the relation $\alpha = \sigma_i/\sigma_o$, where σ_i is the conductivity of the capillary blood and σ_o is the conductivity of the external medium. The smaller the external conductivity the more shallow is the internal potential profile. The effect of the external finite conductivity becomes larger at increasing distance from the current source so that the internal potential profile ends by being determined mostly by the external medium. However, within a distance of 2–3 length constants the potential profile inside the capillary is determined by the exponential term in Eq. A6 in Appendix A.

The internal potential contour also depends on the conductivities ratio $\epsilon = (\sigma_m/\sigma_i) \cdot (\alpha/\delta)$, where σ_m is the specific membrane conductivity and δ is the membrane thickness. (See Glossary.)

The potential field in the external medium is given by Eq. A7, which states that the potential at a given point depends linearly upon the relation σ_i/σ_o and also upon exponential terms containing the membrane resistance and the distance perpendicular to the capillary.

The effect of the finite external conductivity is to increase the length constant, λ. If the length constant is determined from directly measured potential values it may be 5–15% overestimated, which would give a membrane resistance 10–30% too high. Because the error depends on the two parameters ϵ and α an iterative correction of λ and a curve fitting procedure for the best value of α has to be performed for each experiment to obtain the best fitting value of λ. As a routine two iterations were performed to find λ.

A special problem relates to the potential configuration within the capillary close to the tip of the current electrode. It has been theoretically shown that the potential profile in the vicinity of the current source is strongly nonexponential in all three dimensions (Eisenberg and Johnson, 1970) with a much steeper fall. This was also seen by Boulpaep (1972) in a study of the membrane resistance of kidney proximal tubules that have quite low resistances so that the intratubular potential rapidly decays to very low values. The muscle capillary has a length constant that is only 10 times higher than the radius of the vessel, which means that one cannot rely on intracapillary potentials measured at distances closer than ~2 vessel radii from the current source, i.e., 25–30 μm.

The theoretical problems are treated in greater detail in Appendixes A and B, where the correction formulae are presented from which correct length constants can be found. The influence of the extravascular resistance means that determination of the membrane resistance of muscle capillaries requires the following measurements: (*a*) Potential profile within the vessel over a total distance of 200–300 μm, (*b*) potential profile immediately outside the vessel, (*c*) resistivity of frog blood, (*d*) diameter of vessel.

MATERIALS AND METHODS

Preparation

Because most of the experimental details are described in an earlier paper (Crone and Christensen, 1981) where methods for determination of the electrical resistance of endothelium in frog mesenteric capillaries were described, only the main points will be dealt with here, with particular emphasis on the circumstances that are special for work on muscle capillaries.

The experiments were performed on microvessels (arterioles, capillaries, and venules) in the *m. cutaneous pectoris* (sternocutaneous) of the common frog (*Rana temporaria*). The muscle was originally used by Adrian and Zotterman (1926) who described the isolation procedure, and later by Neher and Sakman (1976) and Frøkjær-Jensen (1981). The muscle consists of only two layers of cells (Fig. 1 *b*), which means that it can be transilluminated so that the studies can be performed on the stage of a compound microscope with magnifications up to 320×. A Laborlux II binocular microscope (Leitz, Wetzlar, W. Germany) was used because it has a fixed stage, with the focusing done by moving the microscopic tube. This is, of course, a necessary condition since the stage must be completely fixed once the electrodes are inserted.

The frogs were anesthetized by immersion in 5% urethane solution until their mouth respiration stopped. They were placed on their backs and the skin in the midline from pelvis to sternum was cut. The preparation is fairly simple, cf. Fig. 1 *a*. The skin on the chest of the frog is removed except for a small piece in which the cephalic end of the muscle is inserted. The origin of the muscle is not interfered with, but the fascial investments on either side are cut through, the dissection being stopped near the caudal region where the supplying and draining vessels entered the muscle in the lateral and lower corner. The muscle, which was now isolated except medially where it inserts on the sternum, was reflected downwards so that the inward side now faced upwards (Fig. 1 *b*). The frog was placed on a special frame (which could be fastened to the microscope stage) and supported by sealing wax so that the reflected muscle could be placed over a transparent perspex pillar ~1 cm high and 6 mm in diameter. At the front of the pillar the skin at the insertion was fastened by means of small steel pins to a little rubber plate that had been glued to the front side of the upper border of the pillar. This procedure resulted in a preparation that was vigorously perfused, except along the margins and at the end near the skin insertion. As is seen on a section of the muscle (Fig. 1 *b*) the capillaries lie between the muscle cells, which makes the placement of microelectrodes difficult since one muscle cell must be passed. There are larger vessels that are more accessible and that lie close to the large feeding vessels proximally in the preparation. Sometimes there are superficial vessels here and there in the preparation recognized by their skew course in contrast to the intramuscular capillaries that lie along the muscle fibres.

The isolated muscle is superfused with frog Ringer's solution at room temperature (20°–23°C). It is important that the superfusion be liberal during the measurements to reduce any residual stray resistance between capillary and reference electrode. The superfusate did not contain albumin. The composition of the frog Ringer's solution was the following (in

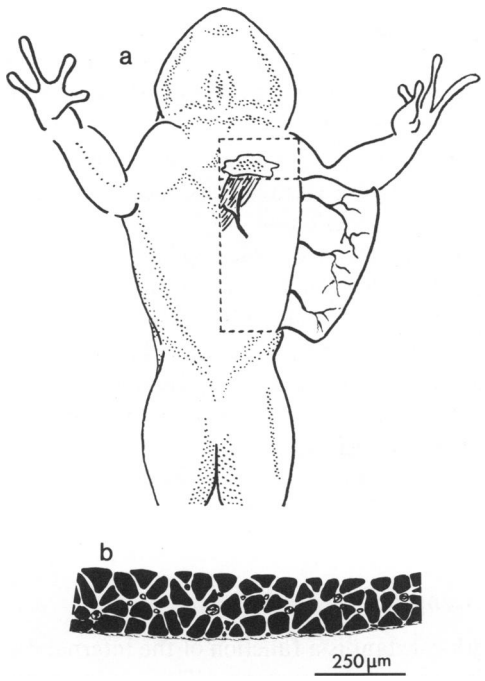

FIGURE 1 (*a*) Sketch of procedure for isolation of *m. cutaneus pectoris* with intact perfusion. The muscle has a cephalic insertion to the skin and caudal insertion to the xiphoid. The vascular supply in the caudal and lateral corner must not be damaged during the dissection. The muscle is reflected forward and placed on a perspex pillar and viewed in transillumination. Further details are given in the main text. (*b*) *M. cutaneus pectoris* of *Rana Temporaria*. A transverse section showing the middle third of the muscle. The upper surface of the section is the everted deep surface uncovered by fascia and connective tissue which is seen at the bottom (the front surface of the muscle in situ). The capillaries close to the upper surface are accessible for electrode impalements. The muscle cells act as insulating cylinders surrounded by conducting interstitial fluid. During the experiments the muscle is covered by a 50–100 μm layer of superfusate. (Microscopic specimen by courtesy of M. Bundgaard, University of Copenhagen.).

millimolar units): Na^+, 110.7; K^+, 2.0; Ca^{2+}, 1.8; Cl^-, 115; and HCO_3^-, 1.2. The osmolality was 215 mOsmol/kg. The micromanipulators and the microscope were fastened to a common aluminium plate placed on a vibration-free table resting on the concrete pillars of the building through holes in the floor. The duration of the experiments was 1–3 h after exposure. If longer times are used the resistance values tend to fall, probably due to inflammatory reactions increasing capillary permeability.

Electrical Measurements

Two electrical circuits were in contact with the tissue. One served to deliver current pulses and consisted of a glass microelectrode filled with 2 M KCl and an agar bridge, 2% agar in 2 M KCl (reference electrode). The tip of the microelectrode was ~0.5–1 μm with a resistance of 5–10 × 10^6 Ω. The constant current generator delivered maximally 0.5 μA against a resistance of 20–30 × 10^6 Ω. Usually current pulses of 0.2–0.4 μA were delivered. It was continuously controlled so that the generator was not overloaded by sudden increases in external resistance.

The potential-measuring circuit consisted of a similar agar bridge and a glass microelectrode, both connected to the input of a high-impedance differential electrometer. The output from the electrometer was fed into a lock-in amplifier in parallel with a storage oscilloscope (OS 4000, Gould Advance, Hainault, Essex, England). The lock-in amplifier (Ortholock-SC 9505, Brookdeal Electronics Ltd., Bracknell, England) permitted reduction of background noise. Via a reference signal, the amplifier locks on the desired frequency and measures only signals that come in with that frequency.

The input impedance of the electrometer amplifier was 10^{13} Ω and the time constant of the system was ~10 ms. Current pulses were delivered with a frequency of 2 Hz and a duration of 250 ms, a time long enough to reach a plateau since the capacitive elements were negligible.

The signals were permanently recorded by means of a Brush recorder with three channels, one of which had double-width pen excursions. Fig. 2 *a* and *b* shows two examples of potential tracings. In one situation the external residual potential was vanishingly small, so that corrections of the length constant were unnecessary, whilst in the other case a clear residual potential is seen. Fig. 3 shows a plot of internal and external potentials against distance from the current electrode, and it is seen that at long distances the course deviates significantly from a monoexponential course by being flatter towards the end. The upper curve in Fig. 3 shows a slight tendency to turn upwards at the end to the right. This reflects the fact that the solution for larger distances "blows up." This is, however, not a problem in the present experiments where measurements are not made at more remote positions. The potential measurements should be confined to an axial region that begins ~300 μm away and ends not closer than 25–30 μm from the current electrode.

The electrical field external to an experimental capillary was investigated in a special series of experiments where an external electrode was placed at various locations along the capillary, and in many positions perpendicular to the capillary, where a current injection electrode was lodged in a fixed position. In this way a contour map of isopotential lines could be constructed. The electrical field was compared with the field described by the Peskoff and Eisenberg theory (Eq. A7 in Appendix A), and it was found that within a region 2–2.5 length constants away from the current source the actual measurements fitted very well with the theory. The experimental results of a field determination are given in Fig. 7, the contents of which is explained in the Appendix. The field was rotationally symmetric around the capillary and identical on either side of the current source.

The distances in the preparation were measured by means of a 20 × 20 grid in one of the eyepieces. It was calibrated, one side of a square was 120 μm at 40× magnification and 15 μm at 320× magnification. The distances between current source and measuring electrode tip was

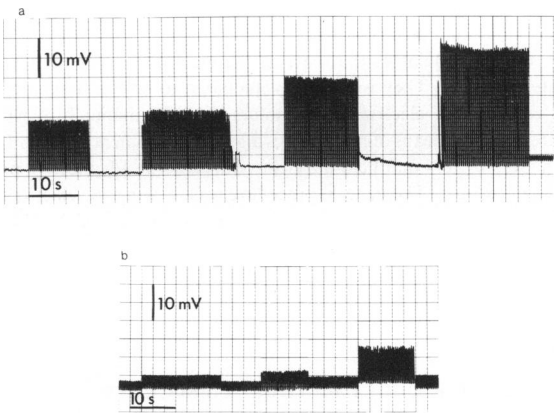

FIGURE 2 (*a*) Chart recorder registration of the intracapillary potentials measured in four different places relative to the current electrode within and just outside microvessel. The vessel was a medium-sized arterial vessel with a high resistance (R_m = 50 Ω cm^2) as reflected in the small residual potentials remaining outside the vessel after withdrawal of the electrode. (*b*) Potential measurements in a postcapillary venule (R_m = 5.0 Ω cm^2). The residual potential remaining on the outside is a substantial fraction of the interior potential necessitating application of analysis involving external field conditions (see Appendix A).

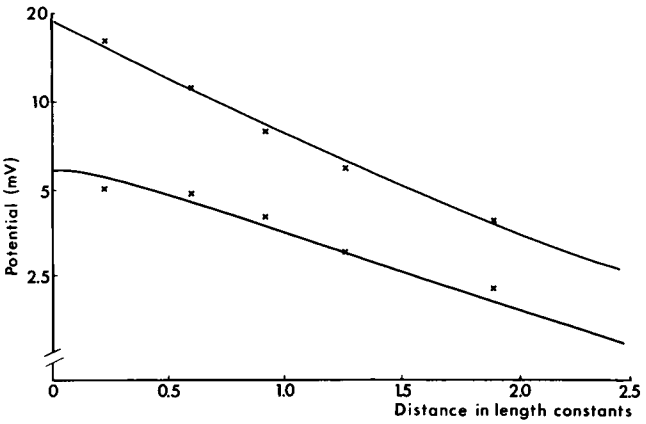

FIGURE 3 Potentials measured inside and just outside the vessel wall in five different positions relative to the current electrode. The crosses (X) are experimental measurements, and the lines show the theoretically calculated potential profiles. In this case the residual outside potential is about one third of the interior potential. If disregarded the length constant would be overestimated by 25%.

determined by Pythagoras' rule when the electrode coordinates were read in Cartesian coordinates.

The nomenclature of microvessels is ambiguous. Arterial capillaries were vessels before the last branching into true capillaries, whilst venular capillaries were the corresponding microvessels formed by merging capillaries. The distinction between arterioles and arterial capillaries is uncertain (as is also the case for true venules and pericytic venules), but it appeared that there were not significant differences between the permeabilities of smaller or larger vessels on the two sides of the true capillaries so that a rigorous distinction is of minor interest.

To reduce the effect of permanent leaks in the capillary wall induced by the potential electrode, measurements were started at remote points from the current electrode and successively made at closer locations. In experiments where the effect of earlier punctures was studied it was found that when a series of measurements were repeated in the same region of a capillary the potentials were clearly lower, reflecting the fact that the penetration by the microelectrode had left a leak. However, with the recommended direction of measurements (starting at remote locations) this problem should be minimized.

The micromanipulators that carried the electrodes were built in the Institute workshop. They were firmly anchored to bronze T-plates. The stands carrying the electrical step motors could be manually moved in *X-Y* directions by means of microdrives allowing movement down to 1 or 2 μm. The step motors that held the electrodes could be advanced in preset steps down to 2 μm. The general procedure was to bring the electrode tip close to the capillary wall by means of the micrometer screws and then to make the final push into the capillary by means of the electrical step motor.

RESULTS

Endothelial Electrical Resistance

Altogether, 49 successful experiments were carried out on various types of microvessels, ranging from arterioles over arterial capillaries, true capillaries, and venous capillaries to venules. As seen on Fig. 1 *b* the capillaries lie under one layer of muscle cells, and for that reason they were rather difficult to work with because of the technical difficulties of making several transcellular penetrations in the same capillary. Therefore most of the measurements refer to vessels either immediately before or immediately after the true capillaries. If measurements on arterial microvessels are pooled an average resistance of 33 Ωcm^2 (SD = 13 Ωcm^2, n = 26) was found.

If, similarly, the measurements on venous microvessels are taken together an average resistance of 23 Ωcm^2 (SD = 7.3 Ωcm^2, n = 20) was found.

Three measurements on true capillaries gave an average resistance of 36 Ωcm^2, not significantly different from the arterial vessels. This result fully corroborates earlier conclusions that true capillaries do not differ much in their permeability from that of neighboring microvessels (Crone et al., 1978). Fig. 4 shows histograms of the results of the measurements of resistance.

One thoroughfare channel was studied. It had a resistance of 103 Ωcm^2 (vessel radius 8 μm, length constant 174 μm).

Length Constants

The length constant is a function of the internal resistance and of the membrane resistance. The results of the determinations of various types of vessels are summarized in Table I which shows that in muscle capillaries the length constant had values between 112 and 135 μm. The radii of the vessels are also given in Table I. The resistivity of frog blood was put equal to 110 Ωcm. This value was chosen because frog plasma has a resistivity of 90 Ωcm and with a hematocrit of 0.30, the resistivity of blood would be ~120 Ωcm. Because the hematocrit in small vessels is lower than the large vessel hematocrit the value 110 Ωcm is somewhat arbitrary, but since it is not possible to determine the small vessel hematocrit in the present experimental approach we chose to use a fixed intermediate resistivity.

DISCUSSION

There are two aspects that deserve special comments and discussion: (*a*) reliability of the measurements, (*b*) the implication of the results for current views about muscle capillary permeability. The suitability of the proposed mathematical model for describing the actual conditions in the muscle slab is discussed in the Appendix A together with the presentation of the details of the model.

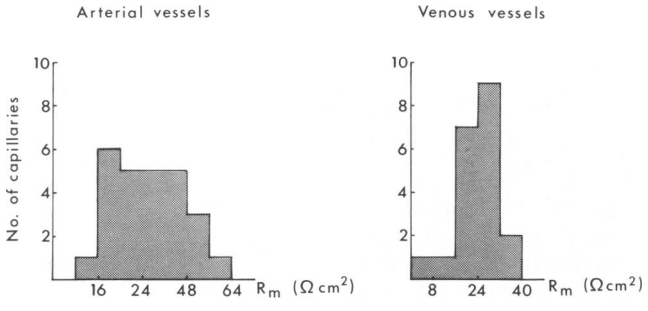

FIGURE 4 Histograms showing the electrical resistance of the endothelium of 26 arterial and 20 venous microvessels reported in the text.

TABLE I
MORPHOLOGICAL AND ELECTRICAL VARIABLES OF MICROVESSELS IN MUSCLE

	Radius	Membrane resistance	Length constant	N
	10^{-4} cm	Ωcm^2	10^{-4} cm	
Arterial vessels	15.1 ± 5.7	33 ± 13	135 ± 38	26
True capillaries	9.9 ± 2.9	36 ± 15	118 ± 37	3
Venous vessels	15.0 ± 6.0	23 ± 7.3	112 ± 29	20

The table shows average figures with the standard deviation. N is number of vessels studied.

Reliability of the Measurements

In our first paper about electrophysiological studies on single capillaries (Crone et al., 1978) we emphasized that there are several pitfalls of such techniques and one must be aware of them as far as they can be sorted out.

Studies on single vessels require exposure of the tissue for a while and it is becoming clear that there is a tendency for the permeability of, in particular, venous vessels to increase with time. This is an old observation, originally made by Rous et al. (1930) in a study of dye escaping from microvessels of rabbit muscle. They showed that venous vessels do leak dye after some time of exposure. Although it is not known with certainty, it is likely that the leakiness does increase little by little. We did not make systematic studies of this, but tried to keep the experimental time as low as possible. Frøkjær-Jensen (1981, 1982) showed some increase in leakiness of venous vessels with time in the same muscle preparation; the increase was, however, rather moderate, ~10–20% within 2–3 h after exposure. He also showed that it probably was due to histamine liberation from mast cells, since blockage of the histamine (H_1)-receptors with promethazine prevented or slowed this development. We did not use pharmacological agents because we wanted to study an unmedicated preparation.

Apart from this potential problem there is no obvious reason why the measurements should not give reliable resistances. There is, of course, a limit to the accuracy with which the vessels' radii can be determined. Because 1 μm is the limit of accuracy in determination of vessel radius, in a preparation like the present one the error in internal resistance may be ~15%. The fact that the substage condensing system was not equipped with lenses that allow focusing in the plane of the preparation meant that full advantage could not be taken of the numerical aperture of the high-power objective, thus reducing the resolving power (Gore, 1982). The uncertainty of the hematocrit value in the microvessels under investigation adds another inaccuracy and increases the error up to, perhaps, 20–25%.

The applicability of the mathematical model to this tissue is, of course, not perfect. In the model we assume homogeneous conditions in the field outside the experimental capillary. This is not wholly true because the extravascular space consists of interstitium alternating with muscle fibres, but we doubt whether refinement of the model will lead to significant changes of the results we have obtained.

If the resistance values are calculated without reference to the model, and a length constant is determined from a semilogarithmic plot of the direct observations disregarding the distributed resistances outside the capillary, a 10–30% overestimation of the actual endothelial resistance would have resulted because of the effect of the flatter late part of the potential vs. distance curve (cf. Fig. 3).

PHYSIOLOGICAL SIGNIFICANCE OF THE RESULTS

Because almost all studies of muscle capillary permeability have been carried out with whole organ techniques and because many potential shortcomings of these techniques have been pointed out (e.g., Michel, 1972) it is of particular interest to compare results obtained with whole organ and single capillary techniques. The present measurements of electrical resistance of single capillaries in muscle tissue allow such a comparison to be made. It is very comforting to conclude that the discrepancies, if any, between whole organ results and single vessel measurements in muscle are small. When the results from single vessel studies of mesenteric capillaries appeared (Crone et al., 1978, Curry, 1979) and it became apparent that the ionic permeability of these vessels was almost one order of magnitude higher than codified results from heart and muscle, one began to wonder whether whole organ techniques were, after all, suffering from serious shortcomings. The present determinations of electrical resistance allow the permeability of the principal ions in plasma to be calculated. For a permeable membrane separating two identical solutions in the absence of an electrical potential difference, the following general expression applies:

$$\frac{RT}{F^2} G_m = \sum_i P_i \cdot c_i \cdot z_i^2,$$

where G_m is the total conductance, R and T have their usual significance and F is Faraday's number (96,490 coul/mol). P_i is permeability, c_i is molar concentration, and z_i is valency.

In the particular case of frog plasma and interstitial fluid being separated by a capillary membrane with negligible potential difference (~1 mV) one can write

$$\frac{RT}{F^2} \cdot G_m = P_{Na} \cdot c_{Na} + P_{Cl} \cdot c_{Cl} + P_K \cdot c_K + P_{HCO_3} \cdot c_{HCO_3}.$$

For the whole experimental series the average resistance was 28 Ωcm^2, equivalent to a conductance of 0.036 $\Omega^{-1} cm^{-2}$.

We assume that the mobility of the individual ions in the hydrophilic pathways in the capillary wall is the same as in

free solution; i.e., there is no selective diffusion restriction or effects of charge upon the diffusion of the small univalent ions. In a rather extensive study of the problem of restricted diffusion of small solutes in continuous capillaries in muscle tissue it was concluded (Crone and Levitt, 1983) that it is unlikely to occur. This implies that the permeabilities are proportional to the limiting conductances. Table II gives the permeabilities for the principal small ions in frog plasma.

Strandell and Shepherd (1968), in experiments on human muscle, found a permeability for sodium of 8.7×10^{-5} cm · s^{-1}, and Trap-Jensen and Lassen (1970) got 5.5×10^{-5} cm · s^{-1}.

Permeabilities at 20°C are ~25% lower than at 37°C, therefore, the temperature correction would bring the present figures even closer to figures obtained in experiments on whole organs (cf. also Yudilevich et al., 1968, and Duran, 1977).

The potassium permeability as calculated above is a little smaller than the figure which Frøkjær-Jensen (1982) found on the same preparation using injections of K^+-enriched solutions and ion-sensitive electrodes. His figure for P_K in arterial capillaries was 7.3×10^{-5} cm · s^{-1} (somewhat higher in venules).

The early results on cat hind limb gave significantly higher values for small ion permeability (Pappenheimer, 1953). Recently, Renkin and Curry (1978) revised the early figures by means of a new theory for transcapillary fluid movement in response to osmotic gradients. The revision brought the early figures down to values which are comparable to the ones which we have found on single capillaries. This correspondence may be taken as an indication that the original osmotic transient figures were, in fact, several times too high, more so for small electrolytes such as Na^+ and Cl^- than for a large molecule such as inulin, the permeability of which was correct.

The fractional capillary surface area that allows passage of current can be calculated, if a fluid with the same resistivity as frog Ringer's solution fills the interendothelial slits. The specific resistivity (ρ_o) of frog Ringer's fluid is 90 Ωcm. If the diffusion path length (Δx) in the interendothelial clefts is 0.9×10^{-4} cm (Perry, 1980) the fractional surface area (A_p/A) is calculated from

$$R_m = \rho_o \cdot \Delta x/(A_p/A),$$

which gives $A_p/A = 2.7 \times 10^{-4}$. Thus, a few ten thousandths of the surface is available for free diffusion. From Perry's (1980) determinations of slit length in muscle capillaries a mean figure of 1,600 cm/cm^2 is calculated. If the average slit width is 200 Å, the total slit area is 32×10^{-4} cm^2/cm^2. Thus, only $2.7 \times 10^{-4}/32 \times 10^{-4} = 8\%$ of the entire slit length is open in muscle capillaries. Estimates of the open fraction of interendothelial slit have been made by Lassen and Trap-Jensen (1970) who reported values between 3 and 18%, depending upon different slit geometries. Casley-Smith et al. (1975) suggested that 5% of the slit was open based upon morphological techniques; Guller et al. (1975), studying the heart, arrived at 20%. Our value of 8% is, of course, only a rough estimate because of uncertainties about the resistivity of the slit pathway. It is at present unknown whether it is similar to that of plasma or whether it is closer to that of the interstitium. It is hard to judge how much diffusion in a labyrinth of ridges in the junction (Wissig and Williams, 1978) augments the resistivity, but it may well have an effect. If the resisitivity which we have used is an underestimation, it means that the fraction of open slit may be >8%.

In brain endothelium the slit is almost completely closed since the electrical resistance is as high as that of a "tight" epithelium (Crone and Olesen, 1982). On the other hand, in mesenteric capillaries ~90% of the slit may be open (Bundgaard and Frøkjær-Jensen, 1982).

At the present state of knowledge it is tempting to assume that variations in permeability between continuous capillaries are due to a greater or smaller part of the interendothelial junction being closed (Lassen and Trap-Jensen, 1970).

There appear to be large variations between permeability figures for individual vessels. This is observed in the present series and in earlier studies on the mesentery (Crone et al., 1978). It has also been observed in other studies on single vessels (Curry et al., 1976). The variation can be due to unavoidable experimental inaccuracies, to different responsiveness of individual microvessels, to the exposure, or to real heterogeneity of permeability in the microcirculation. Heterogeneity of permeability in individual capillaries disappears in whole organ studies. Because the systematic variation of permeability in consecutive segments of microvessels cannot be disclosed by whole organ techniques, there are definite advantages of single vessel experiments and for closer considerations of the structural explanation of capillary permeability they are indispensable, but the greatest potential use probably lies

TABLE II
IONIC PERMEABILITIES IN MUSCLE CAPILLARIES

Ion	Relative conductance	Permeability
		$cm \cdot s^{-1}$
K^+	1.47	5.7×10^{-5}
Na^+	1.00	3.9×10^{-5}
Cl^-	1.52	5.9×10^{-5}
HCO_3^-	0.89	3.4×10^{-5}

The ion permeabilities are calculated from the total membrane conductance as determined experimentally using the relationship between partial conductance and permeability given in the text. The relative conductances are taken from Harned and Owen (1958), Table 6-8-2. The ion concentrations (mmol/l) used in the calculation were Na^+, 104; K^+, 2,2; Cl^-, 74; HCO_3^-, 25, which are the values in frog plasma (Deyrup, 1964). The value of $F^2/RT = 3.82 \cdot 10^3$ at 20°C.

in the possibility of studying rapid pharmacological effects upon capillary permeability.

The most important conclusion from the present results is that whole organ studies on muscle capillary permeability fit well with results of single vessel studies.

GLOSSARY

a	cm	radius of the vessel
r_i	Ωcm^{-1}	internal resistance per unit length of vessel
r_m	Ωcm	membrane resistance per unit length of vessel
r_{abs}	cm	radial distance
r'	ND	r_{abs}/a, radial distance relative to radius
x_{abs}	cm	axial distance
x'	ND	x_{abs}/a, axial distance relative to vessel radius
x	ND	$x_{abs}/\lambda \simeq x'\sqrt{2\epsilon}$, axial distance relative to length constant
R_m	Ωcm^2	specific membrane resistance per square centimeter of vessel surface
R_{abs}	cm	radial distance to current electrode
R'	ND	radial distance to current electrode relative to radius
V'	V	potential
$V(x', r', \Theta)$	$V \cdot \Omega^{-1}$	$= \sigma_i \cdot a \cdot V'$, potential at variable locations from current source
$V_1, V_2, V_3 \cdots$	$V \cdot \Omega^{-1}$	components of intra- or extravascular potentials according to Eq. A5
$u(t)$	A	step function of current at $t = 0$
α	ND	σ_i/σ_o
γ	ND	Euler's constant (0.577)
δ	cm	thickness of the membrane
ϵ	ND	$(\sigma_m/\sigma_i) \cdot (a/\delta) = 0.5 \cdot (a/\lambda)^2$
λ	cm	length constant $= \sqrt{r_m/r_i} = a/\sqrt{2\epsilon}$
σ_i	$\Omega^{-1}cm^{-1}$	specific conductivity of luminal fluid
σ_m	$\Omega^{-1}cm^{-1}$	specific conductivity of membrane
σ_o	$\Omega^{-1}cm^{-1}$	specific conductivity of external medium
ρ_i	Ωcm	specific resistance of 1 cm^3 blood
ρ_o	Ωcm	specific resistance of 1 cm^3 Ringers solution
Θ	ND	angular coordinate.

ND ≡ nondimensional.

APPENDIX A

The Cable Equation for a Vessel Lying in a Medium of Finite Conductivity

A basic condition for the classic cable theory to be valid is that the conductivity of the medium surrounding the cylindrical structure is infinite or, for practical reasons, much greater than that of the inner medium. If this is not the case, the influence of this nonideality must be estimated and corrections made accordingly.

The vessels in *m. cutaneous pectoris* lie between muscle cells as seen on Fig. 1 *b*. The cells are electrically insulating and constitute ~80–85% of the surrounding medium, leaving only a small part of the tissue plus an ~100-μm–thick layer of superfusate as conducting medium. The conducting properties of the fluid layer between the muscle and the perspex pillar upon which it rests are undefined. The thickness of the fluid layer was assessed in a mesenteric preparation mounted in a similar way (Frøkjær-Jensen and Christensen, 1979) and found only to be ~5 μm. The extracellular diffusion velocity of sucrose was reduced to ~20% of the rate of free diffusion in a slab of heart muscle (Suenson et al., 1974, Safford and Bassingthwaighte, 1977); thus there is a significant reduction of extravascular conductivity. The factor α, the ratio between the internal and external conductivity (σ_i/σ_o), found by curve fitting, averaged 10.6 (SD = 3.8; n = 50), somewhat higher than expected from the above diffusion measurements. We chose to smear the interstitial conductance over the total available space, thus reducing the specific interstitital conductance by the factor α. The extravascular conductance is probably not homogeneously distributed in the tissue. Roberts and Scher (1982) describe that in heart muscle the conductivity is several times higher in the direction of the muscle fibres than in the transverse direction; a somewhat similar anisotropy may also apply to striated muscle. However, the general agreement between results and theory offers some justification for our approximation.

The following account of the model that we have used in our data interpretation is based upon the analysis by Peskoff and Eisenberg (1974) for a point source in a cylindrical vessel. The analysis in its original version is very detailed. In the following we give an abbreviated description with particular reference to the circumstances in a muscle preparation, but the Peskoff and Eisenberg report should be consulted for further details. The Glossary recapitulates the terminology used in the following.

It is profitable to use cylinder coordinates and use nondimensional variables. x' is the distance in the axial direction, relative to vessel radius, a (Fig. 5), $x' = x_{abs}/a$ where x_{abs} is the physical variable. $r' = r_{abs}/a$ is the radial variable relative to the radius, and θ is the angle. The point source of current is located at (0, R', 0), where $R' < 1$. R' is the radial distance to current source relative to the radius, $R' = R_{abs}/a$. According to Peskoff and Eisenberg, (1973, 1974) a point source in a cylindrical structure where current is switched on at time $t = 0$ creates a potential V, which is specified by the following Poisson equation (A1), boundary conditions (A2, A3), and initial conditions (A4). The parameters ϵ and α give ratios of conductances as defined in the Glossary.

$$\frac{1}{r'}\frac{\partial}{\partial r'}\left(r'\frac{\partial V}{\partial r'}\right) + \frac{1}{(r')^2}\frac{\partial^2 V}{\partial \theta^2} + \frac{\partial^2 V}{\partial (x')^2} = \frac{-1}{r'}\delta(x')\,\delta(r' - R')\,\delta(\theta)\,u(t) \quad \text{(A1)}$$

$$\frac{1}{\epsilon}\frac{\partial V^-}{\partial r'} = \frac{1}{\epsilon\alpha}\frac{\partial V^+}{\partial r'} = V^+ - V^- + \frac{\partial V^+}{\partial t} - \frac{\partial V^-}{\partial t} \quad \text{(A2)}$$

$$V(x', r', \theta, t) = 0 \text{ at } x' = \pm\infty \text{ or } r' = \infty \quad \text{(A3)}$$

$$V(x', 1^+, \theta, 0^+) = V(x', 1^-, \theta, 0^+). \quad \text{(A4)}$$

The three-dimensional δ-function in Eq. A1 represents the location of the current source (0, R', 0) and the unit step function $u(t)$ represents the

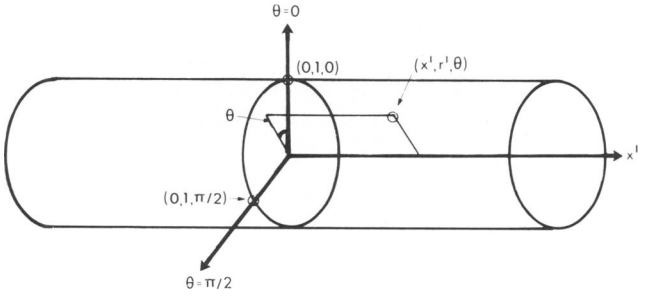

FIGURE 5 Illustration of the system capillary cylinder and surroundings which is described mathematically in Appendix A. The symbols are defined in the Glossary.

current turned on at $t = 0$. The units for $u(t)$ are amperes, and the scaling for V is $V = a \cdot \sigma_i \cdot V'$, where V' is the potential in volts. The boundary condition (A2) expresses continuity of the normal component of a^2 times the current density crossing the membrane. The superscripts + and − represent the conditions just outside and inside the membrane, + with time means just after current injection. The second part of A2 links the membrane current and the electrical properties of the membrane. Boundary condition (Eq. A3) assumes zero potential at infinity: $V = 0$ at $x' = \pm\infty$ or $r' = \infty$. The initial condition (Eq. A4) expresses that no potential difference ($V^+ - V^-$) can appear instantaneously across the membrane, because the membrane capacitance needs a finite time to accumulate charge.

This system of equations has been solved by Peskoff and Eisenberg (1974), and the solution for small values of ϵ, i.e., relatively high membrane resistance at steady state, are given in their Eqs. 3.18 and 3.28. The two Peskoff and Eisenberg equations are printed in Appendix B where it is explained how these rather uninterpretable equations can be rewritten in physically interpretable terms by an expansion in different orders of ϵ as in Eq. A5. The axial variable $x' = x_{abs}/a$ in Eqs. A1–A4 is substituted by the far-field variable $x = x_{abs}/\lambda \simeq x' \sqrt{2\epsilon}$, which is a more convenient nondimensional expression.

$$V(x, r') = \epsilon^{-1/2} \cdot V_0(x, r') + \epsilon^{1/2} \log \epsilon \cdot V_1(x, r') + \epsilon^{1/2} \cdot V_2(x, r') + \epsilon^{3/2} \log \epsilon \cdot V_3(x, r') + \epsilon^{3/2} \cdot V_4(x, r') + \cdots \quad \text{(A5)}$$

Decomposing the first two terms of the exact Peskoff and Eisenberg solution, Eq. 3.18, in the manner indicated in Eq. A5 gives the following result for $r' < 1$ (internal potential):

$$V_0(x, r') = \frac{\sqrt{2}}{4\pi} \cdot e^{-x}$$

$$V_1(x, r') = -\frac{\alpha\sqrt{2}}{16\pi} \cdot e^{-x}$$

$$V_2(x, r') = \frac{\sqrt{2}}{8\pi}\left\{[1.25 - (r')^2 - (R')^2 - \alpha(\gamma - 1 - 0.5 \cdot \log 2)]\, e^{-x} - \frac{\alpha}{2} e^{x}(1 - x) \cdot E_i(-x) + \frac{\alpha}{2} e^{-x}(1 + x)\, E_i(x)\right\}.$$

Taylor expansion, where E_i is an exponential integral, gives

$$V_2(x, r') = 0.056\,\{[1.25 - (r')^2 - (R')^2 + 0.77 \cdot \alpha]\, e^{-x} + \alpha\,[(0.58 + \log x) \cdot (0.33\,x^3 + 0.033\,x^5 + 0.0012\,x^7 + \cdots) + x - 0.45\,x^3 - 0.068\,x^5 - 0.0029\,x^7 - \cdots]\}. \quad \text{(A6)}$$

The set of equations for V_0, V_1, and V_2 together constitutes Eq. A6. Decomposing the first term in the exact Peskoff and Eisenberg solution, Eq. 3.28, one obtains for $r' \geq 1$ (external potential):

$$V_0(x, r') = 0$$

$$V_1(x, r') = -\frac{\alpha\sqrt{2}}{8\pi} \cdot e^{-x}$$

$$V_2(x, r') = -\frac{\alpha\sqrt{2}}{8\pi}[(2\gamma - \log 2 + 2 \log r')e^{-x} + e^{x} \cdot E_i(-x) - e^{-x} \cdot E_i(x)].$$

Taylor expansion gives

$$V_2 = -0.056 \cdot \alpha\,[(0.46 + 2 \cdot \log r') \cdot e^{-x} + 2 \cdot (0.58 + \log x) \cdot (x + 0.17\,x^3 + 0.0083\,x^5 + 0.00020\,x^7 + \cdots) - 2x - 0.61\,x^3 - 0.038\,x^5 - 0.0010\,x^7 - \cdots]. \quad \text{(A7)}$$

The set of equations for V_0, V_1, and V_2 together constitutes Eq. A7. Because only the first terms of the exact solutions are worked out Eqs. A6 and A7 are approximations.

The near field just around the electrode needs a special treatment. The potential profile axially and radially is extremely steep, and the position of the current electrode relative to the vessel wall is here of great importance. In all cases this problem is small about two radii away from the current electrode. For the locations outside the field described above, the model is absolutely not valid (i.e., within very short distances and for large distances as explained). It is seen that for $\alpha = 0$ (infinite external conductance) the classical result is obtained: exponential decay of the internal potential and negligible potential field on the outside.

Example. Typical values of the parameters are $a = 15\ \mu m$; $\lambda = 150\ \mu m$; $\epsilon = 0.5\,(a/\lambda)^2 = 0.005$; $\epsilon^{-1/2} = 14.14$; $\epsilon^{1/2} \log \epsilon = -0.38$; $\epsilon^{1/2} = 0.071$; $\epsilon^{3/2} \log \epsilon = -0.0019$; $\epsilon^{3/2} = 0.00035$.

$$V_{in}(x) = (1.60 + 0.014 \cdot \alpha)e^{-x} + 3.98 \cdot 10^{-3}\alpha[(0.58 + \log x) \cdot (0.33\,x^3 + 0.033\,x^5 + 0.0012\,x^7 + \cdots) + x - 0.45\,x^3 - 0.068\,x^5 - 0.0029\,x^7 - \cdots] \quad \text{(A8)}$$

$$V_{out}(x, r') = 19.2 \cdot 10^{-3} \cdot \alpha \cdot e^{-x} - 3.98 \cdot 10^{-3} \cdot \alpha[2 \cdot (0.58 \cdot \log x) \cdot (x + 0.17\,x^3 + 0.0083\,x^5 + 0.00020\,x^7 + \cdots) - 2x - 0.61\,x^3 - 0.038\,x^5 - 0.0010\,x^7 - \cdots] - 7.96 \cdot 10^{-3} \cdot \alpha \cdot \log r' \cdot e^{-x}. \quad \text{(A9)}$$

In Eq. A8 the radial distances r' and R' to the potential and current electrode are neglected because they are irrelevant in the physical situation.

The inner potential (Eq. A8) is seen to consist of two terms. For small values of x the exponential part is of major importance, but for large x the non-exponential term becomes the dominating one. This is illustrated on Fig. 6. From the expression (A9) describing the external potential it is seen that its magnitude is directly proportional to α. It consists of an exponential term in x, a nonlinear term in x, and a term in x and r', describing the decay of the potential in the direction perpendicular to the vessel.

Fig. 6 shows that overestimate of the length constant results if the influence of the outer potential field is disregarded. The error is squared in the expression for the membrane resistance $R_m = r_i\lambda^2 \cdot 2\pi a$ and a correction is obviously needed. In each experiment an iteration is performed with respect to the two variables ϵ and α. The first value of $\epsilon = 0.5\,(a/\lambda)^2$ is determined from the measured vessel radius a and the apparent value of λ, obtained from a plot of experimentally determined intracapillary potentials at various distances from the current source. A good guess of the value of α can be obtained from the relation between the inner potential and the potential just outside the capillary (Fig. 2*a* and *b*) since

$$\alpha \simeq \frac{2}{\epsilon \cdot \log(\epsilon)} \cdot \frac{V_{out}(0, 0)}{V_{in}(0, 0)}.$$

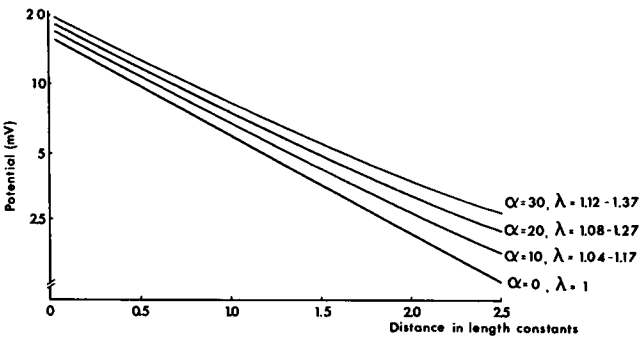

FIGURE 6 Calculated profiles of the interior potential for different values of the relative conductivity ($\alpha = \sigma_i/\sigma_o$) for the case $\epsilon = 0.005$. For $\alpha = 0$, the outer medium conductivity is infinite, and the potential profile is a monoexponential function. The units on the abscissae apply to this situation ($\alpha = 0$). For larger values of α (decreasing conductivity of the outer medium) the profile tends to deviate from a monoexponential course, and the length constant, λ, will increasingly be overestimated as seen in the three examples, if corrections are not made according to the model analysis.

The larger the potential on the immediate outside of the capillary is relative to the internal potential (at the same axial coordinate) the larger the external resistance, which again corresponds to a high value of α. The mean value of α was 10.6, but it does vary from experiment to experiment depending on the structure of the tissue and the effectiveness of the superfusion. The error of λ depending on ϵ and α can be calculated, λ accordingly corrected, and a new ϵ found. A new value of α is then obtained from a computer curvefitting program. As a routine two iterations were performed. Fig. 3 shows how well potential curves can be fitted to the measured values. The upper potential curve is calculated from Eqs. A5 and A6; the lower curve from Eqs. A5 and A7.

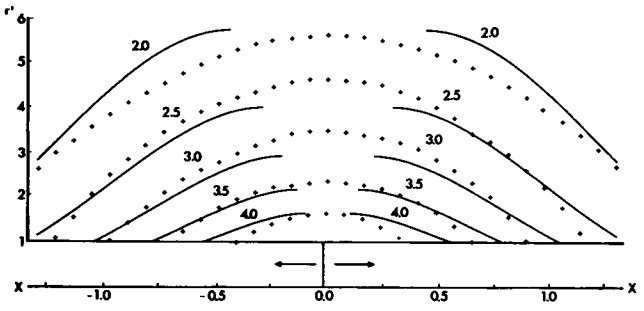

FIGURE 7 Map of the electrical field outside a vessel in a medium of finite conductivity. The lines at the bottom of the coordinate system represent the capillary with a current electrode placed at 0-coordinate on the abscissae. The distances on the abscissae are measured in length constants (x), and the distances on the ordinate (r') are measured in multiples of the vessel radius (1 is the vessel wall). Current pulses of 0.25 μA create an intravascular potential of 15–20 mV at the tip, which declines to either side from zero (not shown on the figure). The potential outside the microvessel declines in three dimensions. A two-dimensional plot of the external potential field, being rotation symmetric around the long axis of the vessel, is shown on the figure. Isopotential lines of 2.0, 2.5, 3.0, 3.5, and 4.0 mV are shown. The crosses (+) represent isopotentials determined from field measurements. The fully drawn lines show the computer calculated isopotentials in a simulated external medium, according to the theory of Peskoff and Eisenberg. The lines are generated by the means of Eq. A9 using fixed values for α and for the potential at the current source (0, 0). The indicated five values for isopotential contours were chosen and r' was found from the model for varying values of x.

Eq. A7 describes a two-dimensional potential field. To illustrate the agreement between theory and experiment, we have made several mappings of the extravascular potential field in response to current injection into the lumen of a vessel and compared it to the field described in Eq. A7. Fig. 7 shows an example, and the fit is satisfactory. This test of the theory was performed in a number of separate experiments with very satisfactory agreement, so that the Peskoff and Eisenberg treatment seems to be directly applicable to the experimental situation in muscle.

APPENDIX B

As described in the main text and in Appendix A the model used rests heavily upon the formal analysis by Peskoff and Eisenberg (1974). Because their original report is not easily available we give here two important equations from their paper: Eqs. 3.18 and 3.28 which are solutions to the system of equations (A1–A4) in Appendix A for small values of ϵ at steady state.

Internal Potential

Peskoff and Eisenberg's Eq. 3.18 describes the potential in the far field inside the cylinder for $r' < 1$:

$$V(x, r') = \frac{1}{2\pi\sqrt{2\epsilon}} e^{-x} + \frac{\sqrt{2\epsilon}}{8\pi} \cdot \left\{ e^{-x} [1.25 - (r')^2 - (R')^2 - \alpha(\gamma - 1) - \frac{\alpha}{2} \log \epsilon/2] - \frac{\alpha}{2} e^{x} (1 - x) E_i(-x) + \frac{\alpha}{2} e^{-x} (1 + x) E_i(x) \right\} + \cdots .$$

External Potential

Peskoff and Eisenberg's Eq. 3.28 describes the far field potential outside the cylinder, for the radial variable in the range $1 \leq r' \ll \epsilon^{-1/2}$.

$$V(x, r', \theta) = -\frac{\alpha}{4\pi}\sqrt{\frac{\epsilon}{2}} \cdot \left[2e^{-x}\left(\gamma + \log\sqrt{\frac{\epsilon}{2}} r'\right) + e^{x} E_i(-x) - e^{-x} E_i(x) - \frac{\epsilon\alpha}{2\pi^2} \sum_{n=-\infty}^{\infty} e^{in\theta} \int_0^{\infty} \frac{dk}{k^2} \cos kx \left[\frac{K_n(kr') I_n(kR')}{I_n'(k) K_n'(k)} - 2\left(\gamma + \log\frac{kr'}{2}\right)\delta_{n0} \right] \right] + \cdots .$$

In the Eqs. E_i are exponential integrals; I_n and K_n are modified Bessel functions.

Interpreting the equations in physical realities is difficult, but as shown by Peskoff and Eisenberg they can be rewritten in a number of physically interpretable terms in orders of ϵ using singular perturbation analysis. The problem specified by Eqs. A1–A4 in Appendix A can be decomposed into a number of problems each with a physical meaning corresponding to a single term in an expansion of the potential in orders of ϵ, and it is shown that each term in the Peskoff and Eisenberg Eqs. 3.18 and 3.28 is a solution to one of the physical situations.

The orders of ϵ chosen to make the expansion are those appearing in the exact solution and it is verified that this is the appropriate expansion that leads to Eq. A5. The individual terms appearing when decomposing the

exact solution this way are recognized by inspection of Eqs. A6 and A7 and comparing with the Peskoff and Eisenberg equations.

Peskoff and Eisenberg have evaluated the terms in the Eq. 3.18 giving the potential inside the cylinder for physiologically relevant figures of ϵ and α, and conclude that the exponential integral term which increases for large x is of major significance relative to the exponential term which decreases with increasing x when $(x/\alpha) \cdot e^{-x} \ll \epsilon$. In a typical case for the muscle capillary with $\alpha = 10$ and $\epsilon = 0.005$, $(x/\alpha) \cdot e^{-x} = \epsilon$ for $x = 4.5$, and for bigger x the value of the expression blows up, contrary to the physical situation. Thus the limit of the far field must be for $x = 2 - 2.5$, which was also the practical limit in the experimental situation. The exact solution for the outer potential, Peskoff and Eisenberg Eq. 3.28, is only valid in the case $1 < r' \ll \epsilon^{-1/2}$ which approximately means $1 < r' < 5$–6 when $\epsilon = 0.005$.

For the outside potential, Eq. 3.28, the exponential integral is relatively more important in the expansion. The exponential integral terms dominate the exponential for values of $x > 1$.

We wish to thank Joseph Patlak, Ph.D., University of Vermont, for demonstrating the dissection of the cutaneous pectoris muscle and J. Frøkjær-Jensen, Ph.D., for help with the preparation. Mr. S.-P. Olesen, M.E.E., held a research fellowship from the Danish Heart Association. Pia Joseffson kindly made the sketch in Fig. 1*a*. Bente Mertz provided expert technical assistance. This work has been supported by the Danish Natural Science Research Council grant 91-3001.

Received for publication 30 November 1981 and in final form 7 October 1982.

REFERENCES

Adrian, E. D., and Y. Zotterman. 1926. The impulses produced by sensory nerve-endings. *J. Physiol. (Lond.)*. 61:151–171.

Boulpaep, E. L. 1972. Permeability changes of the proximal tubule of Necturus during saline loading. *Am. J. Physiol.* 222:517–531.

Bundgaard, M., and J. Frøkjær-Jensen. 1982. Functional aspects of the ultrastructure of terminal blood vessels. A morphometric study on consecutive segments of the frog mesenteric microvasculature. *Microvasc. Res.* 23:1–30.

Casley-Smith, J. R., H. S. Green, J. L. Harris, and P. J. Wadey. 1975. The quantitative morphology of skeletal muscle capillaries in relation to permeability. *Microvasc. Res.* 10:43–64.

Crone, C., and O. Christensen. 1981. Electrical resistance of a capillary endothelium. *J. Gen. Physiol.* 77:349–371.

Crone, C., J. Frøkjær-Jensen, J. J. Friedman, and O. Christensen. 1978. The permeability of single capillaires to potassium ions. *J. Gen. Physiol.* 71:195–220.

Crone, C., and D. G. Levitt. 1983. Exchange of small solutes through the capillary walls. *In* Handbook of Physiology. Section 2. E. M. Renkin and C. C. Michel, editors. American Physiology Society, Washington D.C. In press.

Crone, C., and S. P. Olesen. 1982. Electrical resistance of brain microvascular endothelium. *Brain Res.* 241:49–55.

Curry, F. E., J. C. Mason, and C. C. Michel. 1976. Osmotic reflection coefficients of capillary walls to low molecular weight hydrophilic solutes measured in single perfused capillaries of the frog mesentery. *J. Physiol. (Lond.)*. 261:319–336.

Curry, F. E. 1979. Permeability coefficients of the capillary wall to low molecular weight hydrophilic solutes measured in single perfused capillaries of frog mesentery. *Microvasc. Res.* 17:290–308.

Deyrup, I. J. 1964. Water balance and kidney. *In* Physiology of the Amphibia. J. A. Moore, editor. Academic Press, Inc., New York. 251–314.

Duran, W. N. 1977. Effects of muscle contraction and of adenosine on capillary transport and microvascular flow in dog skeletal muscle. *Circ. Res.* 41:642–647.

Eisenberg, R. S., and E. A. Johnson. 1970. Three-dimensional electrical field problems in physiology. *Prog. Biophys. Mol. Biol.* 20:1–65.

Frøkjær-Jensen, J. 1981. A frog muscle preparation suitable for single capillary studies of K^+-permeability with ion-sensitive microelectrodes. *J. Physiol. (Lond.)*. 316:50P.

Frøkjær-Jensen, J. 1982. Permeability of single muscle capillaries to potassium ions. *Microvasc. Res.* 24:168–183.

Frøkjær-Jensen, J., and O. Christensen. 1979. Potassium permeability of the mesothelium on the frog mesentery. *Acta. Physiol. Scand.* 105:228–238.

Gore, R. W. 1982. Fluid exchange across single capillaries in rat intestinal muscle. *Am. J. Physiol.* 242:H268–H287.

Guller, B., T. Yipintsoi, A. L. Orvis, and J. B. Bassingthwaighte. 1975. Myocardial sodium extraction at varied coronary flows in the dog. *Circ. Res.* 37:359–378.

Harned, H. S., and B. B. Owen. 1958. The physical chemistry of electrolytic solutions. Reinhold Publishing Corp. 3rd ed. New York. 803 pp.

Hodgkin, A. L., and W. A. H. Rushton. 1946. The electrical constants of a crustacean nerve fibre. *Proc. R. Soc. Lond. B. Biol. Sci.* 133:444–479.

Hudlicka, O., B. W. Zweifach, and K. R. Tyler. 1982. Capillary recruitment and flow velocity in skeletal muscle after contractions. *Microvasc. Res.* 23:201–213.

Krogh, A. 1919. The number and distribution of capillaries in muscles with calculations of the oxygen pressure head necessary for supplying the tissue. *J. Physiol. (Lond.)*. 52:409–415.

Lassen, N. A., and J. Trap-Jensen. 1970. Estimation of the fraction of the interendothelial slit which must be open in order to account for the observed transcapillary exchange of small hydrophilic molecules in skeletal muscle in man. *In* Capillary Permeability. The Alfred Benzon Symposium II. C. Crone and N. A. Lassen, editors. Munksgaard, International Booksellers & Publishers Ltd., Copenhagen. 647–653.

Michel, C. C. 1972. Flows across the capillary wall. *In* Cardiovascular Fluid Dynamics. D. Bergel, editor. Academic Press, Inc., New York . 2:241–298.

Neher, E., and B. Sakmann. 1976. Noise analysis of drug induced voltage clamp currents in denervated frog muscle fibres. *J. Physiol. (Lond.)*. 258:705–729.

Paaske, W. P. 1977. Capillary permeability in skeletal muscle. *Acta Physiol. Scand.* 101:1–14.

Pappenheimer, J. R. 1953. Passage of molecules through capillary walls. *Physiol. Rev.* 33:387–423.

Pappenheimer, J. R., E. M. Renkin, and L. M. Borrero. 1951. Filtration, diffusion and molecular sieving through peripheral capillary membranes. *Am. J. Physiol.* 167:13–46.

Perry, M. A. 1980. Capillary filtration and permeability coefficients calculated from measurements of interendothelial cell junctions in rabbit lung and skeletal muscle. *Microvasc. Res.* 19:142–157.

Peskoff, A., and R. S. Eisenberg. 1973. Interpretation of some microelectrode measurements of electric properties of cells. *Ann. Rev. Biophys. Bioeng.* 2:65–79.

Peskoff, A. and R. S. Eisenberg. 1974. A point source in a cylindrical cell: potential for a step-function of current inside an infinite cylindrical cell in a medium of finite conductivity. University of California, Los Angeles. UCLA-ENG-7421: 1–73.

Renkin, E. M., and F. E. Curry. 1978. Transport of water and solutes across capillary endothelium. *In* Transport Across Biological Membranes. G. Giebisch, D. C. Tosteson, and H. H. Ussing, editors. Springer-Verlag, Berlin. 4:1–45.

Renkin, E. M., O. Hudlicka, and R. M. Sheehan. 1966. Influence of metabolic vasodilatation on blood-tissue diffusion in skeletal muscle. *Amer. J. Physiol.* 211:87–98.

Roberts, D. E., and A. M. Scher. 1982. Effect of tissue anisotropy on extracellular potential fields in canine myocardium in situ. *Circ. Res.* 50:342–351.

Rous, P., H. P. Gilding, and F. Smith. 1930. The gradient of vascular permeability. *J. Exp. Med.* 51:807–830.

Safford, R. E., and J. B. Bassingthwaighte. 1977. Calcium diffusion in transient and steady states in muscle. *Biophys. J.* 20:113–136.

Strandell, T., and J. T. Shepherd. 1968. The effect in humans of exercise on relationship between simultaneously measured ^{131}Xe and ^{24}Na clearances. *Scand. J. Clin. Lab. Invest.* 21:99–107.

Suenson, M., D. R. Richmond, and J. B. Bassingthwaighte. 1974. Diffusion of sucrose, sodium, and water in ventricular myocardium. *Am. J. Physiol.* 227:1116–1123.

Trap-Jensen, J., and N. A. Lassen. 1970. Capillary permeability for smaller hydrophilic tracers in exercising skeletal muscle in normal man and in patients with long-term diabetes mellitus. *In* Capillary Permeability. The Alfred Benzon Symposium II. C. Crone and N. A. Lassen, editors. Munksgaard, International Booksellers & Publishers, Ltd., Copenhagen. 135–152.

Tyml, K., C. G. Ellis, R. G. Safranyos, S. Fraser, and A. C. Groom. 1981. Temporal and spatial distributions of red cell velocity in capillaries of resting skeletal muscle, including estimates of red cell transit times. *Microvasc. Res.* 22:14–31.

Wissig, S. L., and M. C. Williams. 1978. The permeability of muscle capillaries to microperoxidase. *J. Cell Biol.* 76:341–359.

Yudilevich, D. L., E. M. Renkin, O. A. Alvarez, and I. Bravo. 1968. Fractional extraction and transcapillary exchange during continuous and instantaneous tracer administration. *Circ. Res.* 23:325–336.